Vol. **131** (2017) *ACTA PHYSICA POLONICA A* No. 5

Proceedings of the 11th Polish–Japanese Joint Seminar on Micro and Nano Analysis, Gniew, September 11–14, 2016

# The Influence of Substrate on Size of Pd Nanoparticles in C–Pd Composites Obtained in the PVD and CVD Processes

K. Sobczak[a,b,*], M. Kozłowski[c] and E. Czerwosz[c]
[a]Institute of Physics, Polish Academy of Sciences, Aleja Lotnikow 32/46, PL-02668, Warsaw, Poland
[b]Faculty of Chemistry, Biological and Chemical Research Centre, University of Warsaw, PL-02089 Warsaw, Poland
[c]Tele and Radio Research Institute, PL-03450 Warsaw, Poland

This paper presents the results of research of C–Pd composite films obtained by the physical vapor deposition and chemical vapor deposition method. These films will be applied as hydrogen sensors. It has been examined whether the substrate has an impact on morphology and topologies of the C–Pd composite and whether the thermal conductivity of the substrate has an impact on the average size of the Pd nanoparticles. Substrates such as $Al_2O_3$, $SiO_2$, Si, and Mo were used, and in the physical vapor deposition process fullerene ($C_{60}$) and palladium acetate were deposited. Some of the samples were examined microscopically, while another part was modified in the chemical vapor deposition process in the presence of xylene. It was found that the average size of the Pd nanoparticles prepared in the physical vapor deposition process is independent of the substrate for all of the substrates used in the present experiment. During the chemical vapor deposition process an increase of the size of the Pd nanoparticles was observed — as expected. What is more, we noticed a weak relation between the size of the Pd nanoparticles and the type of substrate on which the C–Pd composite was deposited.

DOI: 10.12693/APhysPolA.131.1413

PACS/topics: 62.23.Pq, 81.07.Bc, 81.15.Gh, 82.45.Mp

## 1. Introduction

Hydrogen gas is considered to be one of the most promising clean energy carriers that can be used in fuel cells because of its efficiency and environmental friendliness [1]. However, $H_2$ is a highly explosive gas; hence, technological solutions are needed in the construction of sensors that are rapid and sensitive in the detection of this gas. The main components of the studied films are a combination of Pd and porous C. However, such a solution has not yet been applied and was usually limited to Pd and some other compound [2, 3]. Pd is known for its ability to absorb $H_2$ [4] and porous C has high specific surface area [5], which suggests that the combination of these characteristics will significantly increase the possibilities of the detection of hydrogen and will make these films ideal sensors of hydrogen. The nanocrystalline Pd also absorbs $H_2$ [6]; hence nanocrystalline Pd films will be used as active layers in hydrogen and hydrocarbons detectors. The C–Pd films were prepared by using two methods: physical vapor deposition (PVD) and chemical vapor deposition (CVD). The structure and properties of the films prepared by using these processes might depend on parameters such as temperature, time, and substrates. Substrate has a significant effect on the adhesion of the C–Pd film and its morphology. The main aim of this study was to elucidate the influence of the substrate on the average size of the palladium nanocrystallites in the final product of the C–Pd composite.

## 2. Sample preparation and measurements

The C–Pd films were prepared by using PVD process and were modified by using CVD process. In the PVD process, fullerenes and palladium atoms were deposited on $Al_2O_3$, Mo, Si, and $SiO_2$ under a pressure of $10^{-3}$ Pa. Two separate sources were used: one containing fullerene $C_{60}$ in the form of powder (99.9%) and the other with palladium acetate $Pd(C_2H_3O_2)_2$. During the deposition process, the temperature of the substrates was at 60 °C and the time of growth was 10 min. Next, a part of the films were studied by transmission electron microscopy (TEM) and the remaining were modified by using the CVD process. During the second process, the xylene was decomposed over the film surface. The temperature of the substrate was 650 °C and the deposition time was 30 min. Thus, a structure containing Pd nanoparticles (NPs) embedded in the amorphous carbon was obtained. Detailed information about these processes can be found in our previous works [7, 8]. Specimens for planar view electron microscopy observation of the samples were prepared by mechanical stripping of the layer on grid with carbon holey films. The specimen films were studied by using TEM JEOL JEM2000EX, and SEM investigation was performed with a JEOL JSM-7600F.

## 3. Results

Figure 1 presents the appearance an morphology of the typical film obtained after PVD process. Films contained crystalline Pd and $C_{60}$.

Figure 2 presents the film modified through the CVD process. The film also contained Pd crystalline particles but the presence of graphite was noted. Pd NPs

---

*corresponding author; e-mail: ksobczak@ifpan.edu.pl

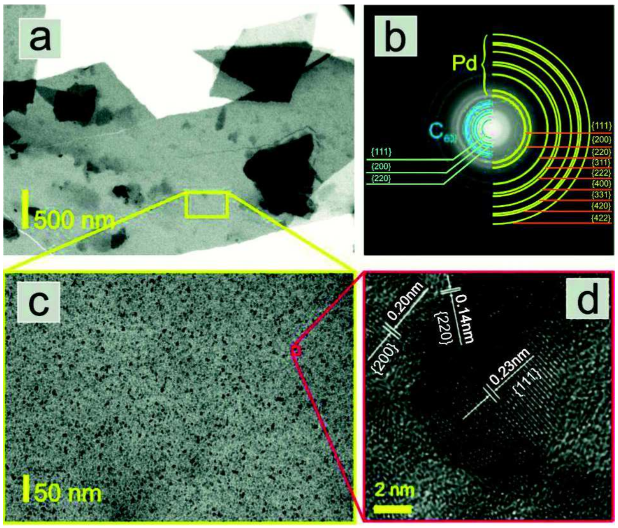

Fig. 1. (a) TEM image of a film prepared in PVD process. (b) The corresponding electron diffraction pattern, in which fullerene $C_{60}$ and the Pd having the fcc structure are identified. In the micrograph (c) enlarged image of the box indicated in (a). (d) High resolution (HR) TEM image of the circle indicated in (c). A single Pd crystallite particle exhibiting the (111) fringes with a lattice spacing of 0.23 nm is presented.

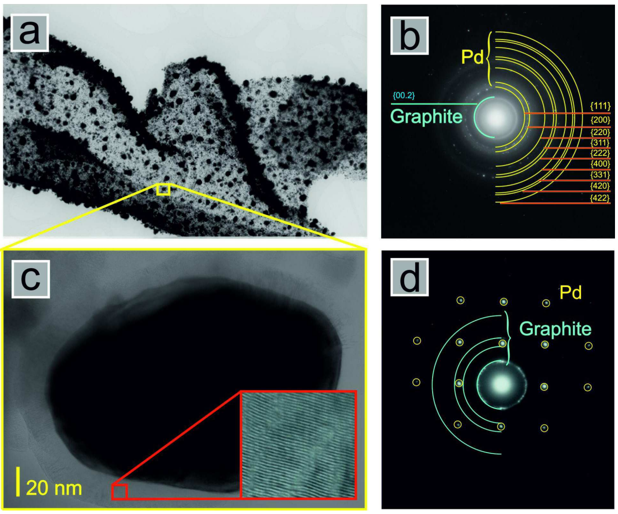

Fig. 2. (a) TEM image of a film obtained after the PVD/CVD processes. (b) The corresponding electron diffraction pattern, where the diffraction rings of graphite and crystalline Pd appear. (c) Enlarged image of the box indicated in (a). A single Pd crystallite is encapsulated with a graphite layer whose lattice fringes are seen in the inset HRTEM image. (d) The corresponding electron diffraction pattern derived from the area of (c).

were encapsulated with graphite layer, as seen in Fig. 2c. More information regarding the structure and morphology of the examined films can be found in our previous papers [9–11]. The high specific surface area of the sensory film will play an important role in adsorption process and provides good sensitivity. Therefore, the type

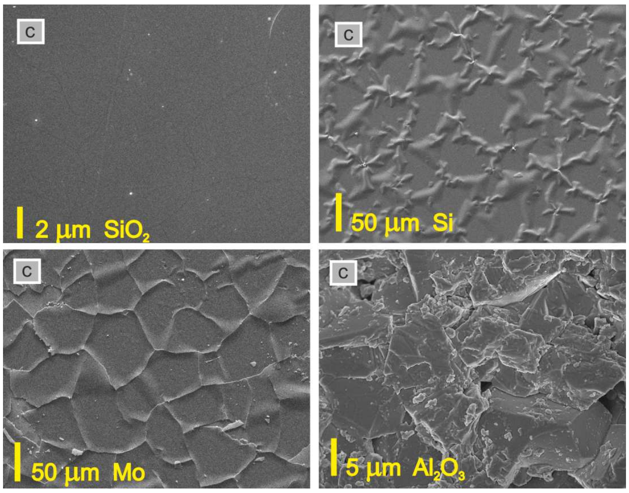

Fig. 3. SEM images of the surface of C–Pd films deposited on different substrates by PVD. The substrate: (a) $SiO_2$, (b) Si, (c) Mo, and (d) $Al_2O_3$.

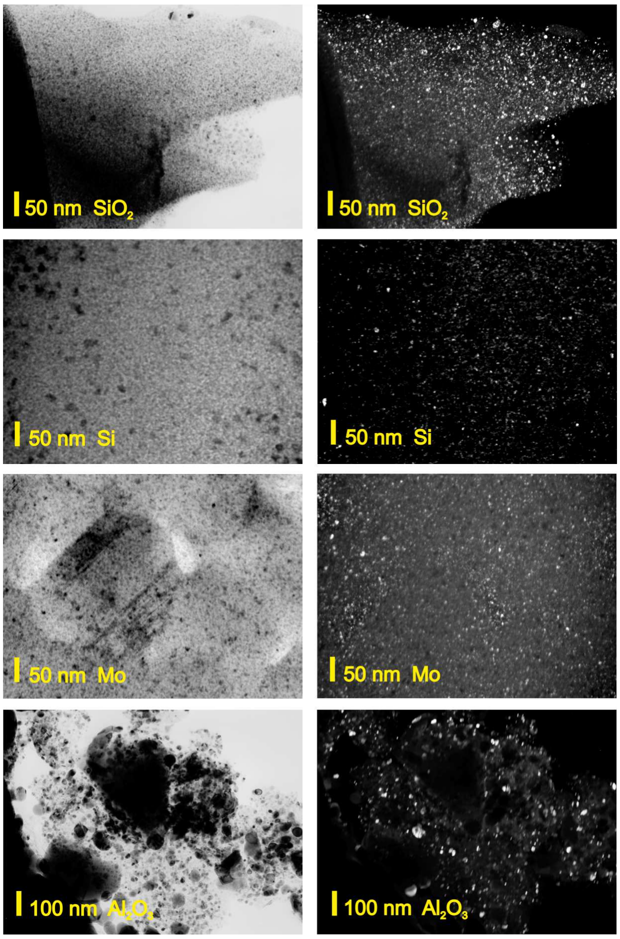

Fig. 4. Bright-field (left) and dark-field TEM images (right) of C–Pd films embedded on different substrates (indicated in the figures) by PVD. Each dark-field image was taken using a diffraction spot from Pd crystallities.

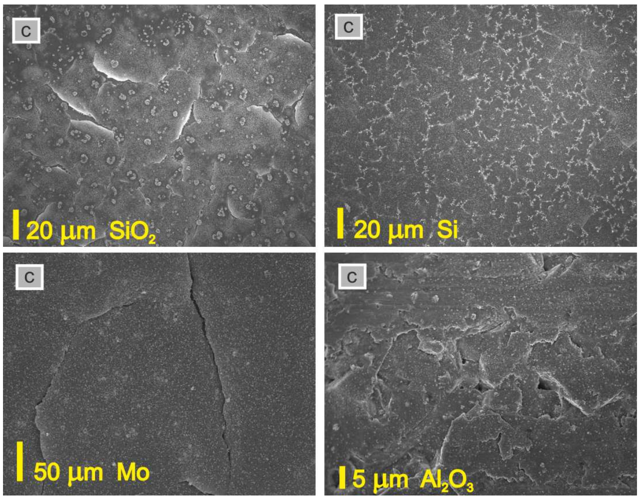

Fig. 5. SEM images of C–Pd surfaces obtained in PVD/CVD process deposited on different substrates: (a) $SiO_2$, (b) Si, (c) Mo, and (d) $Al_2O_3$.

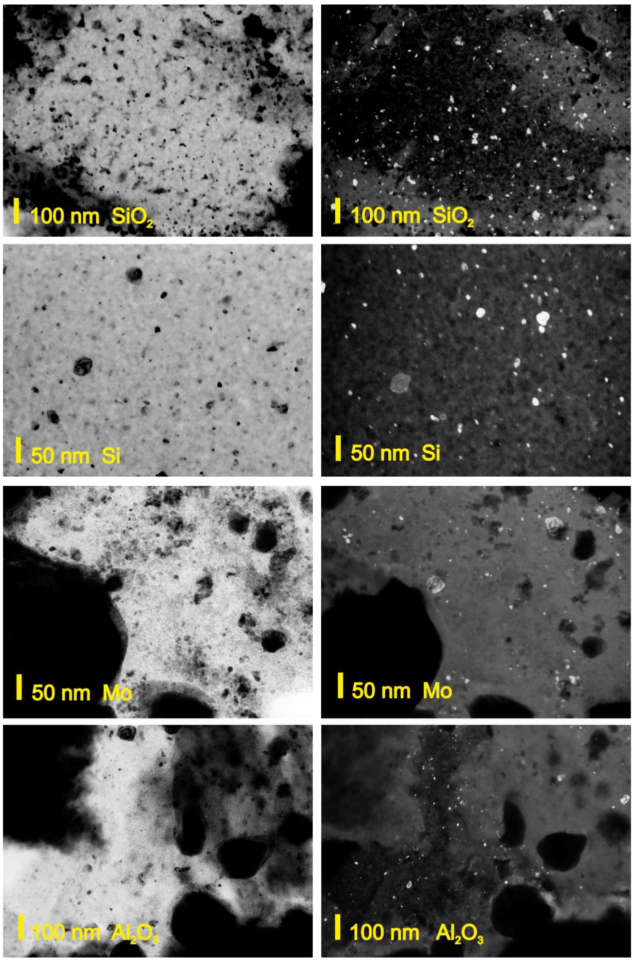

Fig. 6. Bright-field (left) and dark-field TEM images (right) of C–Pd films embedded on different substrates (indicated in the figures) by PVD and modified in CVD process.

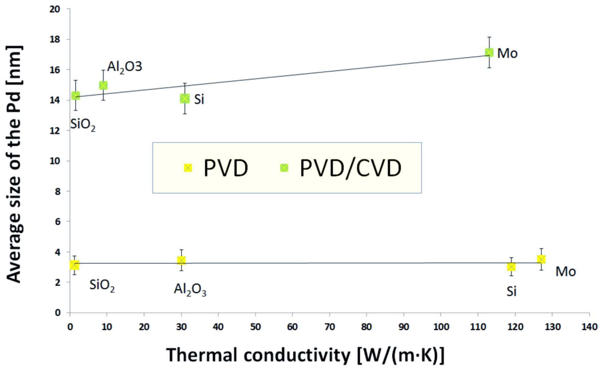

Fig. 7. Relation between the coefficient of thermal conductivity of the substrate and the average nanoparticle size of Pd for both process.

of the substrate impacts the properties of the film in the macroscale. Macroscopically, the PVD films showed no homogeneity.

Figure 3 presents the SEM images of the morphologies of films prepared on different substrates by using PVD process. Figure 3a presents the largest homogeneity in the macroscopic size that was observed on the film deposited on $SiO_2$. In case of other substrates such as Si, Mo, and $Al_2O_3$, differences in surface morphology were observed. The films obtained through the PVD method were characterized by relatively homogeneous distribution of Pd in the C matrix, in the range of hundreds of nanometers.

The homogeneity of the films after the PVD process is well visible in the dark-field images (Fig. 4, right images). In all the four cases, the adhesion of the C–Pd film to the substrate was good. The morphology is different in microscale and nanoscale between the films prepared on different substrates and those modified by the CVD.

Figure 5 presents the SEM images of the macroscopic areas. In the PVD/CVD films, heterogeneous distribution of Pd in C matrix was observed in the range of hundreds of nm.

Figure 6 presents the bright-field and dark-field images of C–Pd films that are modified by using the CVD process. For the quantitative estimation of the size of Pd NPs in the films, size histograms were derived for all the investigated samples. The average size of the Pd NPs was determined by fitting to the log–normal distribution. In order to improve the coverage of surface substrate with the C–Pd film, a heating lamp was used with a temperature of 60 °C during the PVD process and 650 °C during the CVD process.

The average size of Pd in carbon matrix was compared with the coefficients of thermal conductivity of the substrate, and the results are presented graphically in Fig. 7. For PVD processes, the independence of the average size of Pd nanoparticle of the substrate was observed, which is because the substrate was in the thermodynamic equilibrium with the heating element when the PVD process began. A correlation between the coefficient of thermal conductivity and the average size of the nanoparticles was observed in films obtained in the CVD process. The C–Pd films obtained by the CVD process are the modified form of films that were obtained through a PVD process. After the PVD process, films are moved to another system where the CVD process begins. In this process, the substrate is heated to a temperature of 650 °C. Process takes 30 min for all the samples on various substrates, however, the thermal conductivity of the substrate is different. In this case, thermodynamic equilibrium was not obtained between the C–Pd film and heater lamp during the first few min of the process. The higher the thermal conductivity of the substrate, the faster the C–Pd layer reaches the desired temperature. The grain growth is highly dependent on temperature and the annealed time. Therefore, a weak correlation is observed as shown in Fig. 7. The growth of Pd nanoparticle is mainly carried out through diffusion and aggregation [13]. As a result, it is possible to change the annealing time or temperature and obtain the necessary size of the crystallite for all substrates during the CVD process. Thus, as the relationship is so weak, we can control the average size of Pd nanoparticles as well. This information allows for a relatively good control of the average size Pd nanoparticles, and the exercise of sensitive sensory layers for hydrogen PVD film (with average size of Pd $\approx$ 3 nm), [14, 15] and ammonia with PVD/CVD film (with average size of Pd $\approx$ 150 nm) [16].

## 4. Conclusions

The effect of the substrates such as Si, $SiO_2$, $Al_2O_3$, and Mo on the average size of the Pd nanoparticles in the carbonaceous matrix, prepared by using PVD and modified in the following CVD process, was investigated. The independence of the average size of the Pd NPs, of the substrate used in the present experiment was found between the C–Pd films prepared by using PVD method. A correlation between the average size of the Pd NPs and thermal conductivity of the substrate was observed in the C–Pd films modified using CVD method, but it is weak and can be neglected.

## Acknowledgments

This research was co-financed by the ERDF within the Innovative Economy Operational Programme 2007-2013 UDA-POIG.01.03.01-14-071/08-09 and EAgLE Project european action FP7-REGPOT-2012-2013-1. The authors would also like to thank Mrs. J. Radomska and Mrs. H. Wronka for preparing samples.

## References

[1] L. Peraldo Bicelli, *Int. J. Hydrogen Energy* **11**, 555 (1986).

[2] S. Okazaki, S. Johjima, *Thin Solid Films* **558**, 411 (2014).

[3] Z. Hua, M. Yuasa, T. Kida, N. Yamazoe, K. Shimanoe, *Thin Solid Films* **548**, 677 (2013).

[4] T. Graham, *J. Chem. Soc.* **20**, 235 (1867).

[5] G.P. Meisner, Q. Hu, *Nanotechnology* **20**, 204023 (2009).

[6] D. Jose, B.R. Jagirdar, *Int. J. Hydrogen Energy* **35**, 6804 (2010).

[7] M. Kozłowski, R. Diduszko, K. Olszewska, H. Wronka, E. Czerwosz, *Vacuum* **82**, 956 (2008).

[8] E. Kowalska, E. Czerwosz, M. Kozłowski, W. Surga, J. Radomska, H. Wronka, *J. Therm. Anal. Calorim.* **101**, 737 (2010).

[9] E. Kowalska, E. Czerwosz, A. Kamińska, M. Kozłowsk, *J. Therm. Anal. Calorim.* **108**, 1017 (2012).

[10] K. Sobczak, P. Dluzewski, M.T. Klepka, B. Kurowska, E. Czerwosz, *Int. J. Hydrogen Energy* **37**, 18556 (2012).

[11] K. Sobczak, P. Dluzewski, B.S. Witkowski, J. Dabrowski, M. Kozłowski, E. Kowalska, E. Czerwosz, *Solid State Phenom.* **186**, 177 (2012).

[12] E. Kowalska, M. Kozłowski, A. Kamińska, J. Radomska, H. Wronka, E. Czerwosz, K. Sobczak, *Proc. SPIE* **8902**, 89022C (2013).

[13] K. Sobczak, *Int. J. Thermophys.* **36**, 795 (2015).

[14] A. Kaminska, S. Krawczyk, E. Czerwosz, K. Sobczak, M. Kozłowsk, *Sens. Actuat. A Phys.* **196**, 86 (2013).

[15] A. Kaminska, S. Krawczyk, M. Kozlowski, E. Czerwosz, K. Sobczak, *Sensor Lett.* **11**, 500 (2013).

[16] S. Krawczyk, A. Kaminska, M. Kozlowski, J. Radomska, E. Czerwosz, K. Sobczak, *J. Phys. Conf. Ser.* **564**, 012004 (2014).